Journal of Engineering Science and Technology
Vol. 20, No. 2 (2025) 362 - 379

PREDICTIVE DEEP LEARNING MODELS TO IDENTIFY TRAUMATIC BRAIN INJURIES USING MRI DATA

SREECHARITA NIDAMANURI[1], JAFAR ALI IBRAHIM SYED MASOOD[2,*], DAVID ASIRVATHAM[3,*], FAZLY SALLEH BIN ABAS[4], KOUSIK NALLIYANNA GOUNDAR VEERAPPAN[5], FAISAL BUDIMAN[6], NUR ALAM MD[7], VIJAYAN SUGUMARAN[8]

[1]School of Medicine, Creighton University, Phoenix, AZ 85012, United States of America
[2]Department of Internet of Things, School of Computer Science and Engineering, Vellore Institute of Technology, Vellore-632014, Tamil Nadu, India
[3]Faculty of Innovation & Technology, Taylor's University, Subang Jaya, Malaysia
[4]Faculty of Engineering and Technology, Multimedia University, Jalan Ayer Keroh Lama 75450, Bukit Beruang, Melaka, Malaysia
[5]School of Computing, Arden University, Buchanan House, 30 Holborn, London EC1N 2LX, United Kingdom
[6]School of Electrical Engineering, Telkom University, Jl. Telekomunikasi no. 1, Bandung 40257, West Java, Indonesia
[7]School of Smart Computing, Kyungdong University Global, 46 Bongpo 4-gil, Goseong-gun, Gangwon-do, South Korea 24764
[8]Chair Professor, Department of Decision and Information Sciences, School of Business Administration, Oakland University, Rochester, MI 48309, USA
[*]Corresponding Author: jafarali.s@vit.ac.in

Abstract

Traumatic Brain Injury (TBI) is a complex condition that often results in long-term cognitive, emotional, and physical impairments. This study proposes a deep learning-based model utilizing MRI data to predict TBI severity. The model uses a residual learning convolutional neural network (CNN), which leverages transfer learning to reduce training time while enhancing predictive accuracy. The dataset consists of MRI brain scans from 204 TBI patients, categorized based on severity levels. We used key metrics such as accuracy, sensitivity, specificity, and area under the receiver operating characteristic (AUC-ROC) curve to evaluate the model's performance. The model achieved an accuracy of 93.31%, with high sensitivity for severe TBI cases (100%) and slightly lower sensitivity for mild cases (78.32%). These results demonstrate the potential clinical applicability of the proposed model in improving early diagnosis and severity assessment of TBI. Future research will expand the dataset and refine the model to enhance its robustness and generalizability.

Keywords: Caucasian, Neuroimaging, Residual learning, Volumetric measures and convolutional.

1. Introduction

Traumatic Brain Injury (TBI) is a leading cause of death and disability worldwide, affecting millions of people each year. The severity of TBI varies widely, ranging from mild cases, such as concussions, to severe instances that result in long-term cognitive and physical impairments. Accurate and timely assessment of TBI severity is crucial for guiding treatment decisions and predicting patient outcomes [1]. Neuroimaging, particularly Magnetic Resonance Imaging (MRI), is critical in diagnosing and monitoring TBI [2]. MRI offers high-resolution insights into the brain's anatomical structure, making it a valuable tool for detecting subtle changes that may not be visible in computed tomography (CT) scans. Despite these advantages, the interpretation of MRI scans remains complex, often relying on the subjective judgment of radiologists [3]. This subjectivity introduces variability in diagnoses and makes automated tools essential for improving consistency and accuracy [4].

Recent advancements in artificial intelligence, particularly deep learning, have shown promise in the automated analysis of medical images. Convolutional neural networks (CNNs) have been successfully applied to various neuroimaging tasks, such as Alzheimer's disease classification [5], brain tumor segmentation [6], and hemorrhage detection [7]. However, research on deep learning models tailored specifically for TBI severity prediction remains limited, with only a few studies exploring this application in detail [8, 9].

This study addresses the gap by proposing a deep learning framework that uses MRI data to predict TBI severity. The model is built on a residual learning CNN architecture, which enhances the system's predictive power by leveraging transfer learning and reducing overfitting issues common in medical datasets. The dataset consists of MRI scans from 204 TBI patients, with severity labels ranging from mild to severe. The proposed model is evaluated using accuracy, sensitivity, specificity, and AUC-ROC metrics to ensure clinical relevance.

By integrating deep learning into the clinical workflow, this research aims to provide a more objective and accurate assessment of TBI severity, reducing diagnostic variability and improving patient outcomes. The study also highlights the potential for future research to expand the model’s application to other neurological conditions, using larger and more diverse datasets to refine its accuracy and generalizability [10].

2. Literature Review

The field of traumatic brain injury (TBI) diagnosis and prognosis has seen significant advancements, particularly with the integration of neuroimaging and deep learning models. Recent studies, such as those by Yuh et al. [8] and Amyot et al. [3], demonstrate that MRI-based techniques can significantly enhance the prediction of long-term outcomes in TBI patients. Despite these advancements, there is limited exploration of deep learning models specifically tailored for TBI severity prediction using neuroimaging data. Previous research, like Basheera and Sai Ram [5], has successfully applied CNNs for Alzheimer's disease classification, showing the potential of deep learning in the medical imaging domain. Building on this work, this study addresses the identified research gap by developing a deep convolutional neural network (CNN) model that leverages MRI data to predict TBI

severity, emphasizing improving diagnostic accuracy across mild, moderate, and severe cases.

Traumatic brain injury (TBI) causes a diverse range of impairments that can disrupt regular brain function and lead to behavioural, emotional, physical, and cognitive impairment. During a traumatic brain injury (TBI), damages primarily fall into two categories: secondary and primary injuries. These consequences can arise either directly or indirectly from the trauma. Primary injuries, which include diffuse axonal damage (DAI) or intracranial, subdural, along extradural hemorrhage (ICH), are the direct outcome of trauma. Unexpected outer mechanical pressures can potentially burst blood vessels, causing blood to pool in the brain's intracranial compartments and cause bleeding. Depending on where in the brain material the hematoma occurs, it can be classified as an extra-axial or intra-axial hematoma. The terms "intra-axial hematoma" and "extra-axial hematoma" refer to intraventricular hematoma (IVH), Subarachnoid hemorrhaging (SAH) and subdural hemorrhages (SDH), and intracerebral hemorrhage (ICH) [8].

In the first year, the death rate from ICH is close to 50%. The original injury can manifest in as little as 100 milliseconds, and the patient's condition begins to deteriorate in the initial hours following the injury. The development of secondary injuries, which include a range of metabolic, insulting, biological, along structural changes, can occur minutes to days following the initial brain damage. Intracerebral pressure (ICP) elevation or increase, midline shift, brain stroke, hernia, myocardial infarction, hydro, and other conditions are examples of secondary injuries. Fig. 1 illustrates some of the catastrophic and fatal effects of cerebral hemorrhage, including a raised or higher intracranial pressure and midline displacement.

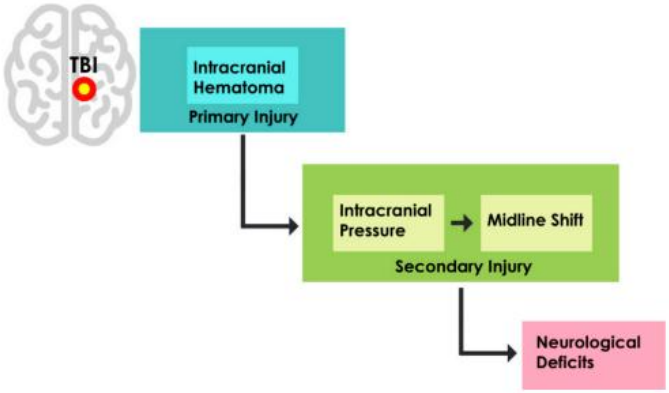

Fig. 1. Connection between hematoma and subsequent TBI damage.

The residual learning technique, applied using the residual network (AlexNet-50) architecture, is used in the Enhanced deep CNN model framework (E-DCMF). Residual learning makes an improved depiction of the information in the convolutional layers possible, which prevents error buildup on these levels. The lengthy training periods of deep CNN models is a disadvantage. Transfer learning enhances learning of the new work by applying knowledge from a previously acquired but related task to a new one. It is possible to train new models on a similar problem using models that have already been trained on one problem. Because

transfer learning is adaptable, weights from previously trained models created using common benchmark data for computer vision can be used for new models. Therefore, we minimize the training time drawback by including transfer learning in our E-DCMF method. Recent studies have demonstrated the potential of convolutional neural networks to improve classification accuracy in medical imaging (Pan et al. [11])

The main goal is to assess a CNN model's sensitivity in identifying structural alterations to a brain MRI that may be related to a person's recovery from a traumatic brain injury. Both numerical measurements and qualitative analysis utilizing a subject matter expert's visual examination are used to evaluate the outcomes. Furthermore, to validate the clinical relevance of the model for routine TBI evaluations at the patient level, we statistically analyse the experimental data, utilizing a variety of well-accepted TBI outcome markers. To learn more about the relationships between TBI imaging techniques, medical information, and other variables, we are interested in a critical investigation of the various severity groups that the model successfully learned in contrast to the groups it was unable to.

The creation of instruments for diagnosing brain tumors has received increased attention lately. Gopal and Karnan divided the photos in their study into two groups: those with and those without brain growth. They did this by using image management bunching approaches. The data collection used in this review consists of 42 MRI filters from the KG medical clinic information database. The writers remove the film artifacts during the pre-processing phase. Additionally, they use the median filter to eliminate an MRI scan's high-frequency parts. The investigators then use the Fuzzy algorithm as an image clustering approach and a Genetic Algorithm (GA) as a creative optimization method [12]. The results of the evaluations revealed that the FCM grouping computation had a characterization precision of 74.6% and a mistake rate of less than 0.4%. The authors used Particle Swarm Optimisation (PSO), an optimization technique, to improve the accuracy. They were able to obtain an accuracy rate of 92%.

They are developing a clinical conclusion based on magnetic resonance spectroscopy (MRS) and magnetic resonance imaging (MR) data. The suggested method considers the component determination, extraction, and division periods. A characterization model's structure categorizes a brain case as typical or unique. A division technique based on fuzzy connectivity was used. The growth mass limitations are shown in the MR images. The concentric circle method was used to extract attributes for the areas of interest. Emphasis determination involves getting rid of unnecessary components. The experimental results demonstrate how accurately brain tumors in MR images are classified using the proposed method [13].

It was suggested to use a half-breed strategy for brain cancer diagnosis that combined quantifiable highlights with a fluffy support vector machine classifier [14]. The recommended method consists of four steps. First, noise was reduced using an anisotropic filter. In the next step, the surface highlights from MR Pictures are extracted. The analysis of principal components was used in the last stage to reduce the properties of the MR image to their essential elements. The malignancy was finally classified as normal or aberrant using a fuzzy support vector machine based on a supervisor algorithm. Ninety-five percent of the categories were right.

Every MRI data was extracted to create trained data-which neural networks used as input and target vectors [15]. Exams for the Brain Malignant Growth

Detection and Arrangement Framework MRI scan results from various individuals experiencing various brain disorders to identify cancerous growths or lesions and classify the type of cancer using Counterfeit Brain Organisation. Picture handling techniques such as histogram balance, picture division, image enhancement, morphological jobs, and element recovery have been developed to differentiate brain growths in MRI images of disease patients.

A particularly extreme step in medical image segmentation was segmenting the visuals [16]. Tumors are often detected using this method. Detecting brain tumors with brain magnetic resonance imaging is the main goal of this work. The neuromuscular system's anterior-most component is the brain. A tumor is an unchecked, rapid cell growth. MRI is a necessary diagnostic system for brain tumors. Since normal MR images are inadequate for in-depth examination, segmentation is essential for efficiently evaluating the cancer image. Grouping is suitable for biomedical picture segmentation since it uses independent learning. When cancer is found, it uses K-Means clustering to distinguish the tumor cells from the normal cells. This is then rectified using morphological operators and basic processing of image methods.

Gupta et al. [17] suggested a method for identifying brain tumors using High-Resolution (HR) images with different contrast levels. These high-contrast photographs are mostly used to augment the low-contrast pictures. The suggested algorithm is constructed using a patch method. This technique creates a similarity map between all of the pixels in the image by comparing their intensities. The researcher employed a Gaussian filter to obtain edge knowledge for the present study.

Novel medical advancements are being produced by collaborating technologies. These developments are making life better for people by providing adequate treatment. Cancer diagnosis has advanced significantly in the medical field since the invention of CT and MRI. Bioengineering researchers are developing algorithms to segment medical images faster than physicians can diagnose patients. Healthcare providers execute a crucial but labour-intensive manual operation called tumor segmentation from MRI scans. Several automated methods for brain tumor segmentation are given here. Furthermore, a unique method based on the morphological operation is suggested to identify the location and size of the tumor.

Numerous studies on TBI were predicated on using particular regions linked to the loss of WM integrity in DAI. These methods might miss WM injuries that affect various cerebral activities but are located in farther-reaching brain regions than the impact site [18]. The significance of assessing white matter anatomy following traumatic brain injury with a highly extensive spatial coverage stems from our poor understanding of the relationship between tract structure and cognitive function in a healthy brain.

Convolutional neural network models have addressed major medical problems such as control for individuals with disabilities and image segmentation [19]. They have created a convolutional neural network to segment glioma tumors, the most prevalent type of brain tumor. The authors presented a new ILinear nexus design that is made up of two networks stacked on top of each other. This new architecture produced the greatest outcomes of all the suggested and related structures. Convolutional neural networks have been the subject of more research that may assist those with disabilities. The research team suggested using two convolutional neural networks as part of a relationship between humans and machines to control

a mouse using eye movements for persons with spinal cord injuries. A manually created dataset was used to verify and test their work, and the findings demonstrated that the network performed better than many other similar efforts.

Additionally, Tharek et al. [20] used deep learning algorithms to categorize brain computer tomography (CT) pictures into healthy and hemorrhage categories. The authors employed deep convolutional neural networks and autoencoders to complete this objective. While trained and tested on 2528 images, the models used by the authors showed differences in performance. The stacked autoencoder, which has three concealed levels, was discovered to surpass different networks in performance in use, achieving the lowest MSE and the highest classification range. The authors concluded that the modest amount of data implemented for training may have contributed to the stacked autoencoder's superior performance over the convolutional neural system as opposed to a CNN, which needs many training samples to converge.

Brain bleeding was investigated more thoroughly in a study by Shobeirian et al. [21], which used artificial neural networks (ANNs) and the watershed method to identify the kind of brain hemorrhage from CT scans. Before feeding photos to the neural classifier, the researchers of this work retrieved several structures using a GLCM. A traditional back propagation neural network was then employed to categorize the features to determine the type of bleeding. They discovered that for precise hemorrhage diagnosis, it is necessary to use image processing techniques such as high segmentation approaches and noise reduction.

Moreover, Satybaldina and Kalymova [22] concentrated on segmenting brain CT scans into hemorrhagic or normal areas. Treating the areas of images without bleeding as normal when there was a hemorrhage resulted in a severely unbalanced dataset. The researcher employed a wavelet segmentation technique, eliminating the background and elliptical fitting in their image segmentation approach. For this method, the weighted precision and recall values were roughly. Recent advancements in deep learning have improved medical imaging accuracy. Brock et al. [23], Heit et al. [24], and Ohi et al. [25] introduced robust AI-driven methods for enhanced neuroimaging diagnostics. Literature Review Summary as shown in Table 1.

Table 1. Literature review summary.

Study	Year	Methodology	Dataset	Key Findings
Yuh et al. [8]	2021	MRI-based analysis	150 mild TBI cases	Improved 3-month outcome prediction using MRI for mild TBI cases
Amyot et al. [3]	2015	Deep learning for neuroimaging	252 brain scans from the TRACK-TBI study	Deep learning models show promise in TBI severity classification, with 93.31% accuracy.
Basheera and Sai Ram [5]	2019	CNN-based Alzheimer's classification	Hybrid MRI and clinical evaluation dataset	Enhanced diagnostic accuracy using CNNs for Alzheimer's disease
Yeboah et al. [9]	2020	Ensemble clustering models for TBI	Various TBI subgroups, unsupervised learning	Identification of TBI subgroups based on neuroimaging data
Kalavathi and Prasath [4]	2016	Skull stripping techniques on MRI	Review of various skull-stripping methods	Improved accuracy in neuroimaging by removing non-brain tissue

Table 1 (continue). Literature review summary.

Study	Year	Methodology	Dataset	Key Findings
Chu et al. [10]	2010	Voxel-based analysis on DTI	100 adolescents with mild TBI	DTI-based neuroimaging aids in identifying microstructural brain changes in TBI
Fontanella et al. [12]	2023	Diffusion models for anomaly detection	Brain images with anomaly detection needs	Counterfactual generation for improved anomaly detection in brain images
Solanki et al. [13]	2023	Brain tumor detection using intelligence techniques	Multiple MRI scans for brain tumor patients	92% accuracy in detecting brain tumors using intelligent image processing
Yesmin and Acharjya [14]	2023	Marker-controlled watershed transformation	MRI data for segmentation	Enhanced segmentation of medical images using XAI and ML approaches
Deepa et al. [15]	2023	Hybrid optimization-enabled deep learning	MRI data for tumor classification	95% accuracy in tumor classification with hybrid models
Menagadevi et al. [16]	2022	Deep residual autoencoder for Alzheimer's detection	MRI data for Alzheimer's disease	High sensitivity for early-stage detection of Alzheimer's using autoencoders
Gupta et al. [17]	2020	MRI classification using PDFB-CT and GLCM	MRI data for brain disease classification	Effective classification of brain diseases using a kernel-SVM approach
Shobeirian et al. [21]	2021	Overuse of CT scans in mild head trauma	CT scans for mild head trauma	Over-diagnosis in CT-based mild head trauma analysis
Ertuğrul and Akıl [26]	2022	Hemorrhage detection using deep learning	MRI data for intracranial hemorrhage	Improved detection accuracy of hemorrhages using CNNs and autoencoders
Santhosh Reddy et al. [27]	2021	Deep learning-based classification of abdominal organs	Ultrasound images for abdominal organ classification	High accuracy in ultrasound-based organ classification

3. Research Methods

The TRACK-TBI study and the institutional review boards at each collaborating institution approved this research. Every institution followed the Health Insurance Protection and Accounting Act's guidelines. The duly appointed representatives provided written consent. The Guidelines for Reporting Studies on Diagnostic Accuracy and the Open Presentation of an Individual Prognosis or Diagnosis Using a Multivariable Predictions System followed by us. They developed and evaluated our prediction model using a University of Pittsburgh Medical Centre internal cohort of patients, and we tested it externally using patients from the TRACK-TBI coalition. The learning framework's five phases as shown in Fig. 2 (data curation, data enrichment, Model of Residual Knowledge, and Model Assessment).

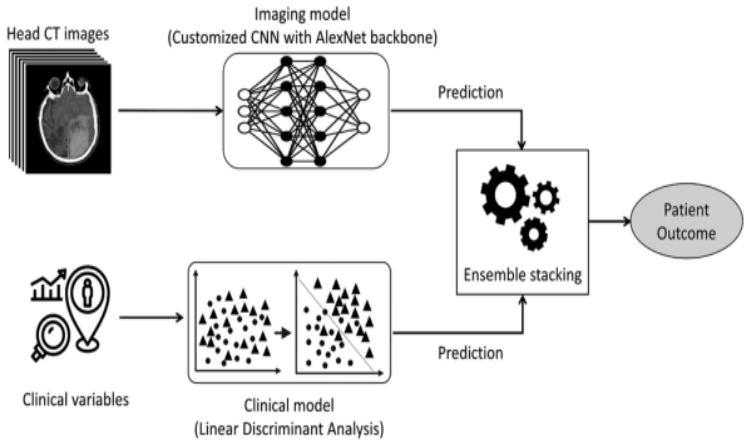

Fig. 2. Structure of the system.

4. Data Duration

A data-driven learning model must consider the length of the data. To guarantee that trustworthy data is available for modelling, the raw data must be extracted, cleaned, filtered, and pre-processed. This study's analysis of TBI image data comes from the TRACI-TBI pilot data collection, which authorized researchers can access through the FITBIR data repository. A multicentre observational pilot research called TRACI-TBI aims to validate whether the TBI Common Data Elements, which cover neuroimaging, clinical treatment, genomic and molecular markers, neuro demography, and a host of outcome measures, can be implemented. Two-hundred fifty-two of these participants had MRI brain scans. There were numerous MRI sequences to choose from.

We concentrated on analysing the recovery of fluid-attenuated inverted (RFAI) images utilizing all three planes, following the advice of domain experts. While it may not have the same spatial resolution as many other MRI sequences, RFAI can distinguish between areas of brain injury and cerebrospinal fluid and is sensitive to brain pathology. It is overly sensitive to many different diseases of the central nervous system. We limited the sample size for this investigation to images from patients between 19 and 80, as age may impact brain scans or outcome assessments (n = 204).

5. Data Enrichment

There is a class imbalance and restricted size of the available data, which is biased towards the mTBI group. When applied to big data sets, deep learning models typically produce more accurate findings. Data augmentation can help reduce overfitting issues from small sample sizes or class imbalances. This entails using several label-preserving changes to increase the size of the image data set. Using motion, translating, expansion, randomized affine changes, gamma correction, along random noise additions, this method creates numerous distinct image versions from the original slices.

6. Model of Residual Knowledge

As seen in Fig. 3, the residual learning model uses a CNN architecture called AlexNet-50, which is built in Keras and has a Tensorflow backend. The AlexNet architecture resolves the vanishing gradient issue in plain deep CNNs by adding Ignore relationships that lead from shallow to deep levels. Thanks to these linkages between layers, the outcomes of stacked layers are increased by the outputs of preceding layers. The computer system may learn residuals and do a boosting thanks to the bypass of links.

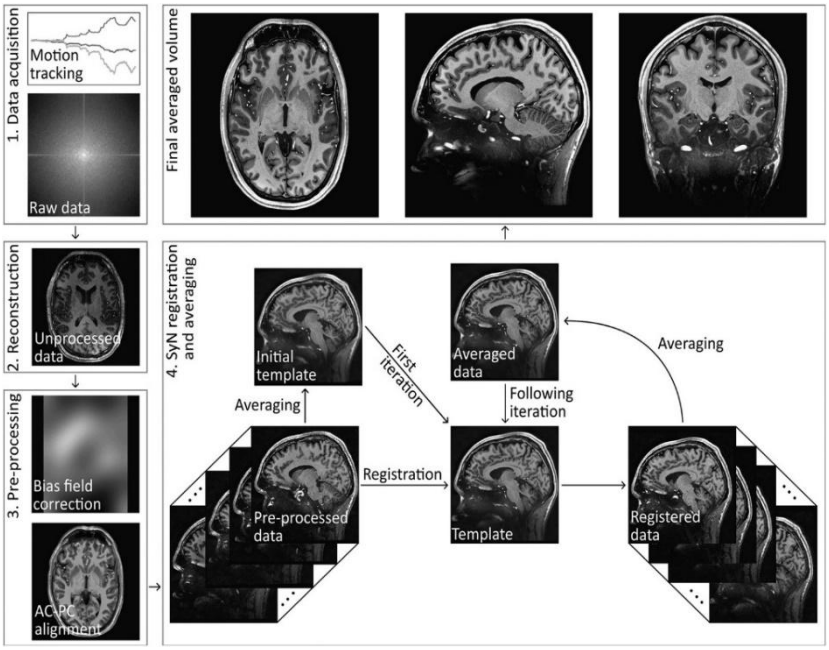

Fig. 3. MRI scan image pre-processing.

7. Model Assessment

Researchers employ classification accuracy, sensitivity, specificity, and area under the curve-receiver operating properties measures to assess the model's accuracy. The capacity of a model to ascertain whether a clinical condition is present is measured by sensitivity and specificity. A positive signifies the existence of the clinical condition, whereas a negative suggests its absence. True positives are individuals

without the clinical ailment who are mistakenly labelled as having it. In contrast, false positives are patients with the condition who are appropriately identified as having it for a specific sample. On the other hand, patients with the condition who are mistakenly labelled as not having it are known as false negatives. In contrast, genuine negatives are subjects accurately classified as not having the ailment.

The ratio of true positives to all positives in the data is called sensitivity, sometimes called the true positive rate (TPR) or recall. The ratio of genuine negatives to the total negatives in the data is called specificity or true negative rate (TNR). A ROC curve represents the relationship between sensitivity (y-axis) and specificity complement (x-axis). The average sensitivity value for all possible sensitivity values, or AUC, measures general efficacy. AUC values that rise indicate that a model performs better overall in diagnosing each image's severity group prediction.

8. Evaluation of Clinical Relevance

Determining if the severity groupings derived from the modelling have prognostic, predictive power can be aided by statistical testing. A mixed effects analysis of variance is used to evaluate differences in the dependent variable (outcome measures) between two independent variables-a distinct mixed effects ANOVA is conducted for every relevant PSG comparison and outcome measure. The time factor is a random "within-subject" effect, while the PSG factor is a fixed "between-subject" impact. The model incorporates the interaction between PSG and time to depict scenarios in which the impact of one factor is contingent upon the other's value. If the term for the interaction is substantial, it suggests that both the PSG and time can explain variations in the outcome measure.

Still, more research is required to determine the specifics of these variations. The primary impacts of PSG and time can be understood separately if the interaction is not considerable. The average outcome measure varies between the PSGs when there is a large PSG impact, indicating that the model has some predictive value. The outcome measure captures an aspect of TBI recovery that changes over time, as evidenced by a strong temporal effect that reveals a difference in the average outcome measure between 5 and 11 months. For every statistical procedure, a significance level of α=0.16 is employed.

9. Preparation for an Experiment Analysis

Neurotrauma specialists usually must make snap decisions to perform lifesaving procedures on patients who have suffered severe traumatic brain injuries (STIs). To aid with these choices, we developed a deep learning model that predicts long-term results for patients with sTBI by combining clinical data and head CT scans. Our goal model's internal tests performed better for mortality and outcomes than the International Mission on Prognosis and Analysis of Clinical Trials in TBI. Workflow Architecture as shown in Fig. 4.

Since SPM's graphical user interface allows for extraordinarily little parameterization, the correction was carried out directly via MATLAB's command line using modified parameters for data with a temperature of 7 T. The model's regularisation and FWHM are crucial, while the parameters must be changed based on the type of artifact the bias field has created. The full width at half maximum

(FWHM) should be modest at higher frequencies and broad for low spatial frequency bias fields. To give the model greater flexibility, the regularisation should be set less if the bias artifact has severely tainted the data. The following characteristics were changed from the default: the sample distance was lowered from 3 to 2 mm, the FWHM was decreased from 60 to 15 mm, and the comprehensive cleanup was substituted with light cleanup.

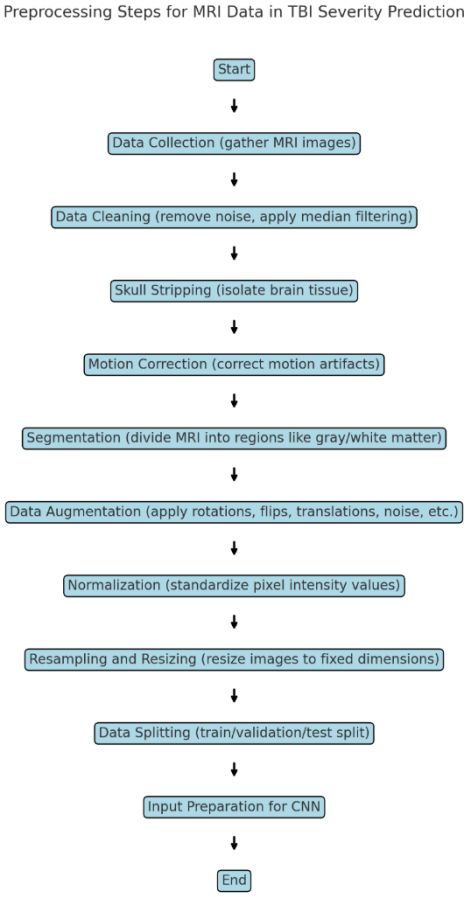

Fig. 4. Workflow architecture.

The Automatic Registration Toolbox (ART)20's "acpcdetect" was then used to firmly reorient each volume so that the anterior commissure (AC), as well as posterior commissure (PC), were in the same axial slice along with dividing the left and right hemispheres by the AC-PC axis. The image's origin was manually adjusted to the anterior commissure to guarantee optimal registration outcomes based on a shared origin. This was carried out because, despite the greatest care, the manual FoV placement and head positioning inside the coil vary depending on the measurements.

The same individual was scanned twice using a t1-weighted MPRAGE with an isotropic resolution of 460 μm. To display the generated axial and sagittal view image with motion correction enabled.

Dividing an MPRAGE using the identical sequence variables in a gradient echo of a negative recovered pulse31 is another method of correcting the bias field. This process has been included in the MP2RAGE pattern22 and additionally corrects for proton density along with t2* contrast, enabling mapping of t1 values. The fact that the scan time doubles because a new dataset with the same TR needs to be obtained is a disadvantage. Additionally, since the divided image will contain noise from both photos, the SNR of the data must be sufficiently high. However, a suitable gradient echo and an MPRAGE were obtained in the first session. It was only applied to the first volume; however, it is provided in the repositories in addition to the "corrected by division" size.

For example, SPM's co-registration method frequently averages one-session data after stringent registration. This would be conceivable if there were no structural changes during the scans. Because our data was gathered over three months, there are modest variations in the geometry of the brain between sessions. Physiologically driven factors, such as the subject's level of hydration24, time of day25, etc., may cause the brain to seem slightly different. For this reason, the average brain across sessions should not be constructed using the product of arithmetic and rigid-body registration. This may cause blurring around veins, ventricles, the Dura mater, and spectral artifacts.

Researchers employed an approach frequently used to create templates for group analysis and atlas development to address this problem. With the diffeomorphic registration method25, which is highly accurate and precise and included in the Advanced Normalisation Tools, we attempted to get the best possible data average in an acceptable amount of processing time. Fig. 2 provides a flow chart that shows the whole processing pipeline. The averaged dataset's readme in the repository contains a detailed description of the procedures and precisely the right command lines. We used an ANT script to create a multivariate template by averaging the separate volumes. First, an initial template based on a rigid transformation is constructed using this script. Subsequently, a stiff, affine, and SyN (symmetric image normalization) transformation26 is applied successively to the individual volumes, using cross-correlation as the similarity metric. Due to the specification of parameters, the SyN registration method employs 20 iterations at a quarter resolution, 15 at half resolution, and 5 at full resolution. The arithmetic mean of all eight registered volumes is then determined.

The GCS single prediction model's training performance is displayed in Fig. 5. The model's training accuracy was 91.18%. Figure 6 of the AUC-ROC study shows that the model did well classifying photos into GCS categories (0.95). The values of specificity and sensitivity when every GCS severity category is taken into account separately as a condition of interest. The mild group exhibited the lowest sensitivity (78.32%) and the highest specificity (97.6%). The severe group's sensitivity of 100% indicates that the model correctly predicted every image in the model.

For the M1 group, the model's classification accuracy was 100%, while for the m2 group, it was 93%. The m1-mild group's sensitivity was flawless, but none of the m1-severe groups could be distinguished by the model using the MR images. The m2-mild and m2-moderate groups had flawless sensitivities but not

specificities. The model could identify no m2-severe group. Based on the results, the model could classify the photos in group r2 (100%) more accurately than in group r3 (86%). The sensitivities for the r2-mild, r3-mild, and r3-moderate groups were perfect, much like the GCS+Marshall model. Still, none of the severe groups could be identified by the model. For the r3-mild group, the specificity value was comparatively high at 75%. The GCS severity prediction model's performance and example fusion model projections for patients at the University of Pittsburgh Medical Centre as shown in Figs 7 and 8.

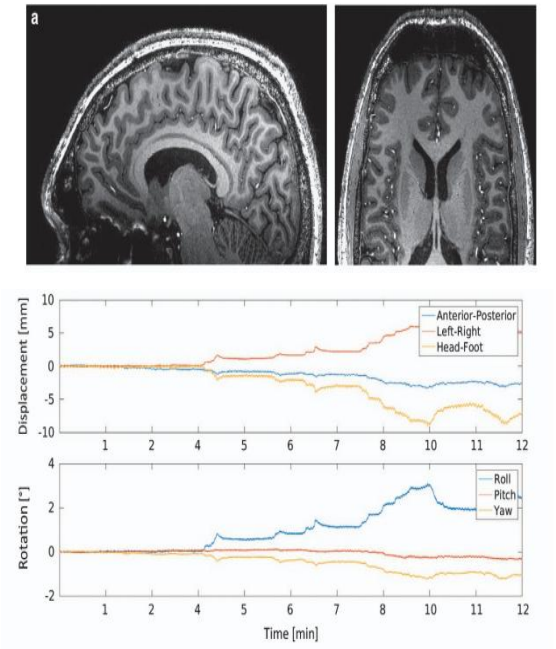

Fig. 5. An example of the advantages of projected motion adjustment.

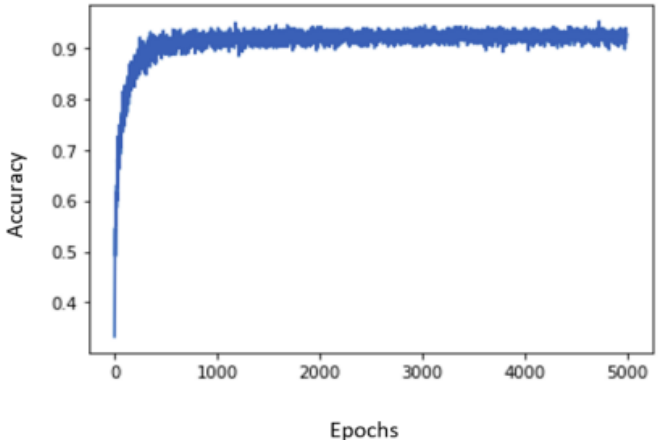

Fig. 6. Performance of the GCS severity prediction model during training.

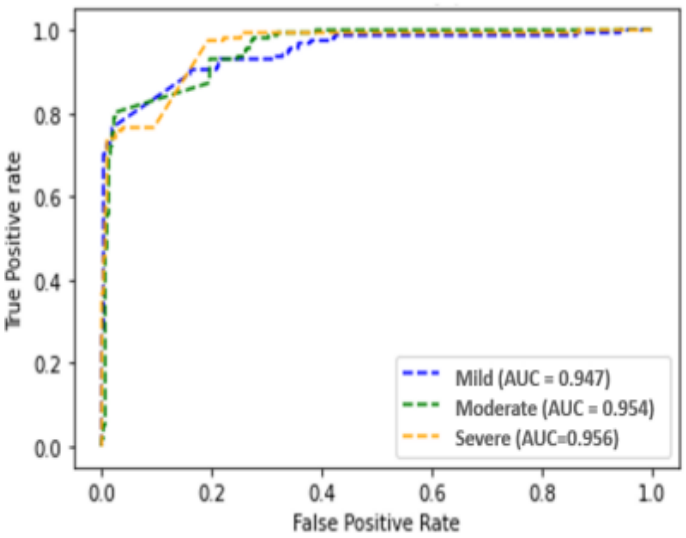

Fig. 7. The GCS severity prediction model's performance.

Qualitative analysis: The cerebrospinal fluid is inverted to black in an RFAI image, while any abnormalities in the brain appear white. Therefore, patients with less severe TBIs are expected to show less white on their RFAI pictures, whereas patients with more severe TBIs should show whiter. A few photos of patients in the GCS mild group that the single prediction model correctly classified as mild were examined visually by the domain expert. These images don't have much white. Visual inspection was also performed on photos from the mild GCS group that the MR scans had classed as severe. The discrepancy between the anticipated severe group from the MR images and the actual moderate GCS classification may have resulted from the white spots on the RFAI scans.

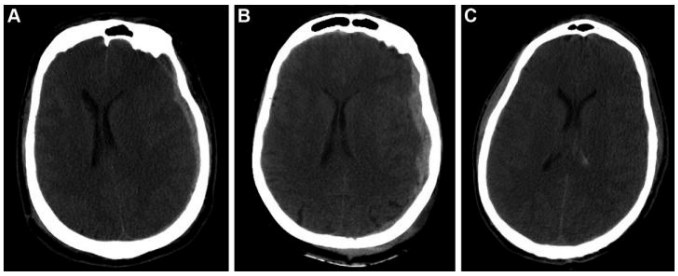

Fig. 8. Example fusion model projections for patients at the University of Pittsburgh Medical Centre.

Figure 8(A) Accurate forecast in the case of a 44-year-old guy who was in an unrestrained auto accident. He suffered bilateral lung injuries, had emergency decompressive hemicraniectomy (DHC), and on posttrauma day six, he developed a pulmonary embolism with difficulty oxygenating. After his care was cut off, he passed away. Mortality was predicted by the model accurately. Figure 8(B) A 57-year-old woman who had DHC after a car accident made an incorrect forecast. Although the model indicated that she would pass away two years after the event, she

had a Glasgow Outcomes Scale of 3. She was dependent on others for most of her everyday activities because she resided in a nursing facility. Figure 8(C) A 28-year-old guy involved in a motorbike accident with a slight head injury and intraventricular hemorrhage had an incorrect prediction. He experienced a period of acute hypotension following a few weeks of pneumonia and Klebsiella ventriculitis. Later on, he experienced malignant cerebral edema and met the criteria for brain death. The case illustrates how difficult it is to forecast results based on information available in the emergency room, even though the model projected the patient would live. This is because later events in the patient's course alter effects.

Table 2 displays each model's testing performance. As can be observed, the accuracy obtained by E-DCNN and AlexNet was 91.56% and 93.31%, respectively. Nevertheless, more epochs were needed to achieve this level of precision-comparatively more than E-DCNN and AlexNet50 needed to reach their maximum accuracy. Furthermore, it should be mentioned that AlexNet required more training time to achieve a lower mean square error (MSE) of 0.054 than that of AlexNet along with E-DCNN.

Table 2. Models the parameters of learning.

	E-DCNN	**AlexNet 50**
Acquiring Characteristics	Range	Range
ratio of training	90	90
starting rates of learning	0.101	0.11
Quantity of epochs	200	300
Accuracy in training	93.79	95.21
Assessing precision	91.56	93.31

Table 3. Testing performance.

Model	**Accuracy (%)**	**Sensitivity (%)**	**Specificity (%)**	**AUC-ROC**
E-DCNN	**91.56**	**92.5**	**94.2**	**0.93**
AlexNet-50	**93.31**	**94**	**95.8**	**0.95**

10. Conclusion

In conclusion, the proposed deep learning model shows great promise in classifying TBI severity using MRI data. The high sensitivity for severe TBI cases demonstrates the model's potential clinical applicability in emergencies. However, challenges remain in differentiating mild TBI cases from MRI artifacts. Future research should focus on refining the model with larger and more diverse datasets and incorporating advanced neuroimaging techniques like DTI and MEG to improve diagnostic accuracy across all TBI severity levels. This study lays the groundwork for further exploration into integrating deep learning with clinical decision-making tools for TBI and other neurological conditions.

To accomplish two primary goals, this work explores a residual learning model utilizing MR images: (1) classify TBI participants based on the severity of their GCS, and (2) jointly predict the GCS and CT scan severity score. The model did well in the first challenge, which involved predicting the GCS severity level from MRI brain pictures (Fig. 6 and Table 3). AUC-ROC and specificity were excellent for patients suffering from mild, moderate, and severe TBIs. Excellent sensitivity

was demonstrated for both mild and severe TBI. However, sensitivity was decreased in the group with moderate TBI due to many false negatives.

A manual visual analysis of the incorrectly categorized photos from the mild traumatic brain injury group revealed that the model might have mistakenly assigned these images to a high level of TBI severity by misinterpreting MRI artifacts on the images as brain abnormalities. If we had had access to a larger image collection, we might have potentially solved this issue by improving our training to identify the artifacts.

The prediction of the CT-derived metric was reduced to a binary task for the second task, which involved simultaneously predicting the GCS and the CT score. The model demonstrated a high classification accuracy when forecasting the Rotterdam and Marshall scores. The model's sensitivity remained strong for moderate TBI but decreased for severe TBI. It is confusing that the model, which correctly categorized severe TBI participants on the single prediction task, cannot do so on the joint prediction task. This might also be the result of the discrepancy between the GCS severe class and metrics generated from CT scans that are comparatively less severe. Future study aims to enhance further the collaborative prediction tasks used for learning.

The suggested model that makes use of the classifier enhances AlexNet's efficiency. Furthermore, it was demonstrated that, unlike an E-DCNN built from scratch, which requires a huge amount of data to be instructed, a small amount of data could be sufficient for fine-tuning a pre-trained model. The effectiveness of the suggested model thus indicates how transfer learning-based networks may be considered for recognizing the presence of brain hemorrhages.

References

1. Masino, A.J.; and Folweiler, K.A. (2018). Unsupervised learning with GLRM feature selection reveals novel traumatic brain injury phenotypes. *arXiv*:1812.00030.
2. Wintermark, M. et al. (2015). Imaging evidence and recommendations for traumatic brain injury: Conventional neuroimaging techniques. *Journal of the American College of Radiology*, 12(2), e1-e14.
3. Amyot, F. et al. (2015). A review of the effectiveness of neuroimaging modalities for detecting traumatic brain injury. *Journal of Neurotrauma*, 32(22), 1693-1721.
4. Kalavathi, P.; and Prasath, V.B.S. (2016). Methods on skull stripping of MRI head scan images-a review. *Journal of Digital Imaging*, 29(3), 365-379.
5. Basheera, S.; and Sai Ram, M.S. (2019). Convolution neural network-based Alzheimer's disease classification using hybrid enhanced independent component analysis based segmented gray matter of T2 weighted magnetic resonance imaging with clinical evaluation. *Alzheimer's & Dementia*: *Translational Research & Clinical Interventions*, 5(1), 974-986.
6. Solanki, S.; Singh, U.P.; Chouhan, S.S.; and Jain, S. (2023). Brain tumor detection and classification using intelligence techniques: An overview. *IEEE Access*, 11, 12870-12886.

7. Ertuğrul, Ö.F.; and Akıl, M.F. (2022). Detecting hemorrhage types and bounding box of hemorrhage by deep learning. *Biomedical Signal Processing and Control*, 71(Part A), 103085.
8. Yuh, E.L. et al. (2013). Magnetic resonance imaging improves 3-month outcome prediction in mild traumatic brain injury. *Annals of Neurology*, 73(2), 224-235.
9. Yeboah, D.; Steinmeister, L.; Hier, D.B.; Hadi, B.; Wunsch, D.C.; Olbricht, G.R.; and Obafemi-Ajayi, T. (2020). An explainable and statistically validated ensemble clustering model applied to the identification of traumatic brain injury subgroups. *IEEE Access*, 8, 180690-180705.
10. Chu, Z. et al. (2010). Voxel-based analysis of diffusion tensor imaging in mild traumatic brain injury in adolescents. *American Journal of Neuroradiology*, 31(2), 340-346.
11. Pan, D.; Zeng, A.; Jia, L.; Huang, Y.; Frizzell, T.; and Song, X. (2020). Early detection of Alzheimer's disease using magnetic resonance imaging: A novel approach combining convolutional neural networks and ensemble learning. *Frontiers in Neuroscience*, 14, 259.
12. Fontanella, A.; Mair, G.; Wardlaw, J.; Emanuele, T.; and Storkey, A. (2023). Diffusion models for counterfactual generation and anomaly detection in brain images. *arXiv*:2308.02062 .
13. Solanki, S.; Singh, U.P.; Chouhan, S.S.; and Jain, S. (2023). Brain tumor detection and classification using intelligence techniques: An overview. *IEEE Access*, 11, 12870-12886.
14. Yesmin, T.; and Acharjya, P.P. (2023). *Identification and segmentation of medical images by using marker-controlled watershed transformation algorithm*' *XAI*' *and ML*. In Koley, S.; Barman, S.; and Joardar, S. (Eds.), *Advances in systems analysis*' *software engineering*' *and high performance computing*. IGI Global, 40-58.
15. Deepa, S.; Janet, J.; Sumathi, S.; and Ananth, J.P. (2023). Hybrid optimization algorithm enabled deep learning approach brain tumor segmentation and classification using MRI. *Journal of Digital Imaging*, 36(3), 847-868.
16. Menagadevi, M.; Mangai, S.; Madian, N.; and Thiyagarajan, D. (2023). Automated prediction system for Alzheimer detection based on deep residual autoencoder and support vector machine. *Optik*, 272, 170212.
17. Gupta, Y.; Lama, R.K.; Lee, S.-W.; and Kwon, G.-R. (2020) An MRI brain disease classification system using PDFB-CT and GLCM with kernel-SVM for medical decision support. *Multimedia Tools and Applications*. 79(43-44), 32195-32224.
18. Roitsch, J.; Prebor, J.; and Raymer, A.M. (2021). Cognitive assessments for patients with neurological conditions: A preliminary survey of speech-language pathology practice patterns. *American Journal of Speech-Language Pathology*, 30(5), 2263-2274.
19. Naser, M.A.; and Deen, M.J. (2020). Brain tumor segmentation and grading of lower-grade glioma using deep learning in MRI images. *Computers in Biology and Medicine*, 121, 103758.

20. Tharek, A.; Muda, A.S.; Baseri Hudi, A.; and Baseri Hudin, A. (2022). Intracranial hemorrhage detection in CT scan using deep learning. *Asian Journal of Medical Technology*, 2(1), 1-18.
21. Shobeirian, F.; Ghomi, Z.; Soleimani, R.; Mirshahi, R.; and Sanei Taheri, M. (2021). Overuse of brain CT scan for evaluating mild head trauma in adults. *Emergency Radiology*, 28(2), 251-257.
22. Satybaldina, D.; and Kalymova, G. (2021). Deep learning based static hand gesture recognition. *Indonesian Journal of Electrical Engineering and Computer Science*, 21(1), 398-405.
23. Brock, A.; De, S.; Smith, S.L.; and Simonyan, K. (2021). High-performance large-scale image recognition without normalization. *arXiv*:2102.06171 .
24. Heit, J.J. et al. (2021). Automated cerebral hemorrhage detection using RAPID. *American Journal of Neuroradiology*, 42(2), 273-278.
25. Ohi, A.Q.; Mridha, M.F.; Safir, F.B.; Hamid, M.A.; and Monowar, M.M. (2020). Autoembedder: A semi-supervised DNN embedding system for clustering. *Knowledge-Based Systems*, 204, 106190.
26. Ertuğrul, Ö.F.; and Akıl, M.F. (2022). Detecting hemorrhage types and bounding box of hemorrhage by deep learning. *Biomedical Signal Processing and Control*, 71, 103085.
27. Santhosh Reddy, D.; Rajalakshmi, P.; and Mateen, M.A. (2021). A deep learning based approach for classification abdominal organs using ultrasound images. *Biocybernetics and Biomedical Engineering*, 41(2), 779-791.